

Nuclear imaging for cardiac amyloidosis

Walter Noordzij · Andor W. J. M. Glaudemans ·
Simone Longhi · Riemer H. J. A. Slart ·
Massimiliano Lorenzini · Bouke P. C. Hazenberg ·
Claudio Rapezzi

Published online: 26 November 2014
© Springer Science+Business Media New York 2014

Abstract Histological analysis of endomyocardial tissue is still the gold standard for the diagnosis of cardiac amyloidosis, but has its limitations. Accordingly, there is a need for non-invasive modalities to diagnose cardiac amyloidosis. Echocardiography and ultrasound and magnetic resonance imaging can show characteristics which may not be very specific for cardiac amyloid. Nuclear medicine has gained a precise role in this context: several imaging modalities have become available for the diagnosis and prognostic stratification of cardiac amyloidosis during the last two decades. The different classes of radiopharmaceuticals have the potential to bind different constituents of the amyloidotic infiltrates, with some relevant differences among the various aetiological types of amyloidosis and the different organs and tissues involved. This review focuses on the background of the commonly used modalities, their present clinical applications, and future clinical perspectives in imaging patients with (suspected) cardiac amyloidosis. The main focus is on

conventional nuclear medicine (bone scintigraphy, cardiac sympathetic innervation) and positron emission tomography.

Keywords Amyloidosis · Nuclear medicine · PET · MIBG · Bone scintigraphy

Introduction

Cardiac amyloidosis is a creepy killer, sneaking into the patient, turning up insidiously with non-specific symptoms, and usually being detected late when the heart is already heavily affected. Awareness is the first step for diagnosis that is further based on imaging techniques and tissue analysis of heart or other tissues. Because of ongoing extracellular deposition of amyloid fibrils, cardiac walls thicken and become stiff. Ultrasound and magnetic resonance imaging (MRI) can detect both thickened ventricular walls and systolic/diastolic dysfunction [1]. However, many other heart diseases can present the same echocardiographic and MRI phenotype. Furthermore, these findings become evident only in a relatively advanced stage of the disease, whereas an early diagnosis is a prerequisite for any efficacious therapy in systemic amyloidosis! So other diagnostic—ideally non-invasive—techniques are needed in order to face the multiple clinical needs of physicians treating patients with suspected or definite amyloidosis. Nuclear medicine has gained a precise role in this context.

Several nuclear medicine imaging techniques have become available for the diagnosis and prognostic stratification of cardiac amyloidosis during the last two decades. The different classes of radiopharmaceuticals have the potential to bind different constituents of the amyloidotic infiltrates, with some relevant differences among the

W. Noordzij (✉) · A. W. J. M. Glaudemans · R. H. J. A. Slart
Department of Nuclear Medicine and Molecular Imaging,
University of Groningen, University Medical Center Groningen,
PO Box 30.001, 9700 RB Groningen, The Netherlands
e-mail: w.noordzij@umcg.nl

S. Longhi · M. Lorenzini · C. Rapezzi
Department of Cardiology, University of Bologna, Bologna,
Italy

S. Longhi · M. Lorenzini · C. Rapezzi
S. Orsola, Malpighi Hospital, Bologna, Italy

B. P. C. Hazenberg
Rheumatology and Clinical Immunology, University of
Groningen, University Medical Center Groningen, Groningen,
The Netherlands

various aetiologic types of amyloidosis and the different organs and tissues involved:

- Serum amyloid P component (SAP) binds in a calcium-dependent way to all amyloid infiltrates, but fails to image cardiac amyloid probably because of its large molecular size [2];
- Aprotinin, a bovine anti-serine protease which binds to amyloid with an unknown mechanism, has also been used in the past to image cardiac amyloid with disappointing results [3];
- Antibodies raised against a common epitope of amyloid fibrils were not able to visualize cardiac amyloid [4];
- Bone-seeking tracers (in particular diphosphonates) image cardiac amyloid of the ATTR type very specifically and early and can be used to differentiate between the amyloid types, since AL amyloid shows only weak or no imaging at all [5]. The nature of this specific binding to ATTR amyloid has not been clarified yet;
- Pittsburgh compound-B labelled with the radionuclide carbon-11 ($[^{11}\text{C}]\text{-PiB}$), derived from the amyloid stain thioflavin, has been recently used as tracer for cardiac amyloid [6] with still inconclusive clinical results;
- Iodine-123 labelled metaiodobenzylguanidine ($[^{123}\text{I}]\text{-MIBG}$) can be used as a functional tracer showing cardiac sympathetic denervation in early stages of amyloid deposition [7].

This review focuses on the background of the commonly used modalities [bone-seeking tracers, $[^{123}\text{I}]\text{-MIBG}$ and positron emission tomography (PET)], their present clinical applications, and future clinical perspectives in imaging patients with (suspected) cardiac amyloidosis.

Nuclear medicine techniques

Radiopharmaceuticals used for diagnostic purposes are administered intravenously. Gamma camera and PET/(CT) camera systems are used to visualize the distribution of radiopharmaceuticals in the body. Both systems detect γ -rays emitted from the patient and transform it into an image. The choice for either system depends on the property of the radionuclide. The choice for a radionuclide depends on the characteristics of the compound (drug, antibody, enzyme) it should be labelled to.

A gamma camera is equipped with a collimator which guides individual γ -rays emitted by the radionuclide. For planar imaging, a collimator is used to transfer only those γ -rays (or photons) which pass in a perpendicular course. This camera system is used to visualize the distribution of, for example, $[^{123}\text{I}]$ and technetium-99m ($[^{99\text{m}}\text{Tc}]$), radionuclides used in imaging cardiac amyloidosis. Despite the

introduction of high-resolution collimators, image quality is rather poor due to limited spatial resolution (approximately 8 mm) and poor statistics of detected photons. Furthermore, planar imaging has low contrast due to the presence of overlying structures that interfere with the region of interest. Single photon emission computed tomography (SPECT) can overcome this superposition and improves sensitivity.

PET is different from conventional nuclear medicine, since these camera systems detect two photons originating from annihilation of emitted positrons with electrons. The detection of both photons is needed to determine the location of the annihilation in the field of interest (for example the thorax). Both photons have to be detected within a certain time window, to consider these two photons as one pair from the same annihilation process. A ring-shaped detector system is needed for this method of photon detection. In contrast to gamma cameras, PET scanners do not need the use of a collimator. As a result, the spatial resolution is approximately 4 mm.

Nowadays, many camera systems are hybrid systems, consisting of either gamma or PET camera combined with multi-detector computed tomography (CT). SPECT or PET and CT are performed in an immediate sequential setting, without changing the position of the patient, providing perfect co-registration of (patho)physiological with anatomical information. Furthermore, the use of low dose CT has additional advantages for attenuation correction. Very recently, hybrid camera systems combining PET with magnetic resonance imaging (PET/MRI) were introduced. The application of PET/MRI in cardiac amyloidosis has not yet been determined.

Bone-seeking tracers for cardiac amyloidosis

Radiolabelled phosphate derivatives, initially developed as bone-seeking tracers, were first noted to localize to amyloid deposits with the visualization of calcifications in amyloid deposits using $[^{99\text{m}}\text{Tc}]\text{-diphosphonate}$ [8]. This observation led to the development of several phosphate derivatives tagged with $[^{99\text{m}}\text{Tc}]$ including $[^{99\text{m}}\text{Tc}]\text{-pyrophosphate}$ ($[^{99\text{m}}\text{Tc}]\text{-PYP}$), $[^{99\text{m}}\text{Tc}]\text{-methylene diphosphonate}$ ($[^{99\text{m}}\text{Tc}]\text{-MDP}$), $[^{99\text{m}}\text{Tc}]\text{-hydroxy methylene diphosphonate}$ ($[^{99\text{m}}\text{Tc}]\text{-HPD}$), and $[^{99\text{m}}\text{Tc}]\text{-3,3-diphosphono-1,2-propanodicarboxylic acid}$ ($[^{99\text{m}}\text{Tc}]\text{-DPD}$).

$[^{99\text{m}}\text{Tc}]\text{-DPD}$ Of all the bone-seeking tracers, $[^{99\text{m}}\text{Tc}]\text{-DPD}$ has been the most studied as possible tracer for cardiac amyloidosis. Currently, this isotope is not approved by the Food and Drug Administration (FDA) and therefore is not available for clinical use in the United States, whereas it is widely adopted in Europe.

The first publication of patients with cardiac [^{99m}Tc]-DPD uptake reported that this phenomenon could be identified in all patients with ATTR amyloidosis and was not present in oncological control patients [9]. In the following published series, [^{99m}Tc]-DPD imaging was performed in 25 patients with cardiac amyloidosis (15 ATTR, 10 AL) confirmed by echocardiogram and endomyocardial biopsy with immunohistochemistry or by genotyping. All 15 ATTR patients had strong myocardial uptake of [^{99m}Tc]-DPD, while no uptake was observed in AL patients [10]. In a further larger cohort of 79 patients where tracer retention was calculated by a heart-to-whole body ratio (H/WB), the diagnostic accuracy of [^{99m}Tc]-DPD scintigraphy was found to be lower due to tracer uptake in about one-third of AL patients with sensitivity 100 % and specificity 88 % using moderate-to-strong uptake as cut-off. Importantly, these studies were performed using a visual scoring (VS) where 0 = no uptake, 1 = mild uptake, 2 = moderate uptake, and 3 = strong uptake. In this second study, the positive predictive value (PPV) and negative predictive value (NPV) for VS 1 were 80 and 100 %, respectively, compared to 100 and 68 % for VS 3. Using a VS 2, ^{99m}Tc -DPD had a NPV 100 % for excluding AL amyloid, while a positive cardiac uptake of [^{99m}Tc]-DPD had a PPV of 88 % for ATTR amyloid [5].

The preferential uptake of [^{99m}Tc]-DPD in ATTR compared to AL amyloid cardiomyopathy remains to be explained, but it is probably related to different amounts of calcium ions available for the binding with the isotope.

[^{99m}Tc]-DPD imaging is now widely used in Europe in the field of amyloidosis, and other clinically relevant data have been produced:

- [^{99m}Tc]-DPD uptake occurs also in carriers of the TTR mutations before the acquisition of a clear echocardiographic and electrocardiographic phenotype [11] and in asymptomatic elderly people with echocardiographic and biopsy-proven wild-type TTR-related cardiomyopathy [12];
- Heart tracer retention (calculated as heart-to-whole body ratio) is related to the severity of cardiac amyloid deposition as expressed by LV parietal thickness and by LV systolic/diastolic dysfunction [11];
- [^{99m}Tc]-DPD myocardial uptake is of prognostic value for predicting major adverse cardiac events (MACE, for example myocardial infarction and sudden cardiac death), either alone or in combination with LV wall thickness [11].

A recent study performed in a large number of patients not only confirmed the high sensitivity of [^{99m}Tc]-DPD scintigraphy in detecting TTR-related amyloidotic cardiac involvement but also showed that SPECT imaging can detect diffuse skeletal muscle uptake as a hitherto

unrecognized site that merits investigation as a target organ in ATTR amyloidosis. This extensive soft-tissue uptake may lead to a reciprocal reduction in bony uptake due to masking of the bones [13].

[^{99m}Tc]-HDP Other diphosphonates were also used to study cardiac amyloidosis. Earlier studies comparing the different diphosphonate bone-seeking agents did not show any significant differences in diagnostic accuracy in bone diseases [14, 15]. Therefore, probably the behaviour of the different diphosphonates is also the same in patients with amyloidosis. [^{99m}Tc]-HDP was used in a group of patients with ATTR amyloidosis in different phases of their disease (carriers of an amyloidogenic TTR mutation, proven ATTR amyloidosis with echocardiographically defined cardiac amyloidosis, and ATTR amyloidosis without echocardiographically defined cardiac amyloidosis), to relate the findings to echocardiography, ECG, and cardiac biomarkers. All patients with proven cardiac amyloidosis showed high diphosphonate heart uptake. So did eight out of 19 patients with ATTR without cardiac amyloidosis signs on echocardiogram. Correlations were found between heart-to-skull ratio on planar bone scintigraphy with troponin T and heart-to-whole body ratio with left ventricular mass index. In this study, bone scintigraphy detected cardiac involvement in patients with ATTR amyloidosis prior to echocardiographic evidence. Cardiac uptake on the bone scan correlated with severity of cardiac involvement using echocardiography, ECG, and biomarkers [16].

[^{99m}Tc]-PYP Another phosphate derivate that has been studied extensively for cardiac amyloidosis is [^{99m}Tc]-PYP. A number of a case reports since 1980 demonstrated myocardial uptake of [^{99m}Tc]-PYP in amyloid patients. Despite this, [^{99m}Tc]-PYP scintigraphy has not been validated as a method in identifying cardiac amyloid due to variable sensitivities, lack of identification of amyloid subtype in earlier studies, and failure of a quantitative method for detecting myocardial amyloid [17–20]. More recently, two studies provided interesting data, potentially able to induce a clinical diffusion of this tracer.

The first study introduced a quantitative method, the ‘PYP score’, to assess the clinical utility of [^{99m}Tc]-PYP for the evaluation of cardiac amyloidosis [21]. In this study, 13 subjects with heart failure due to amyloid (1 AL, 1 AA, 11 ATTR) and 37 subjects with heart failure due to non-amyloid causes were analysed. PYP score, defined as the ratio of myocardial mean counts to ventricular cavity mean counts, was found to have a sensitivity of 84.6 % and specificity of 94.5 % for distinguishing cardiac amyloidosis from non-amyloid causes of heart failure.

Recently, the second study reported the use of [^{99m}Tc]-PYP SPECT in 45 subjects (12 AL, 23 ATTR) with biopsy-proven amyloidosis [22]. Cardiac retention was assessed

with both a semi-quantitative visual score (VS) in relation to bone uptake (0 = no cardiac uptake to 3 = high uptake greater than bone) and by quantitative analysis by drawing a region of interest (ROI) over the heart corrected for contralateral counts and calculating a heart-to-contralateral ratio (H/CL). The degree of cardiac tracer retention in the heart correlated with left ventricular wall thickness and mass. Subjects with ATTR cardiac amyloid had significantly higher semi-quantitative cardiac VS than the AL cohort, as well as a higher quantitative score. The authors concluded that [^{99m}Tc]-PYP cardiac imaging may be a simple, widely available method to identify subjects with ATTR-type cardiac amyloidosis. Despite potentially relevant limitations (selection of patients with more advanced cardiac amyloid and V122I mutation), this study suggests that [^{99m}Tc]-PYP (already available in the USA) can help physicians in recognizing TTR-related cardiac amyloidosis and in discerning ATTR from AL amyloid

In summary, labelled diphosphonates play an important role in the typing of amyloidosis and in diagnosing heart involvement in patients with ATTR amyloidosis with confidence. Cardiac involvement in ATTR patients may be diagnosed earlier with bone scintigraphy in ATTR patients compared to echocardiography.

PET tracers for imaging cardiac amyloidosis

Although PET/CT has advantages over conventional nuclear medicine modalities (improved spatial resolution and potential of quantitative measurements), the role of PET/CT in cardiac amyloidosis is still limited. Currently two studies and one case report, using three different radiopharmaceuticals, involving cardiac amyloid deposits have been published. The first study used *N*-[methyl- ^{11}C]2-(4'-methylamino-phenyl)-6-hydroxybenzothiazole ([^{11}C]-PiB), which is a tracer developed to visualize β -amyloid in Alzheimer's disease. The aim of this study was to visualize and quantify cardiac amyloid deposits in ten (both AL and ATTR) patients with systemic amyloidosis and to compare the distribution of [^{11}C]-PiB to five healthy control subjects. To determine the relationship of [^{11}C]-PiB to myocardial blood flow (MBF), myocardial perfusion imaging was performed using [^{11}C]-acetate. Cardiac [^{11}C]-PiB uptake was heterogeneous in patients, but significantly higher compared to controls, with all control subjects negative for cardiac tracer uptake. There was no relationship between [^{11}C]-PiB and MBF [6].

More recently, another study using a radiopharmaceutical which was developed for imaging β -amyloid in the brain, [^{18}F]-florbetapir, was published. Tracer uptake in fourteen patients with biopsy-proven cardiac amyloidosis was compared to five control subjects [23]. In concordance

with the [^{11}C]-PiB study, all amyloid patients and none of the control subjects showed cardiac [^{18}F]-florbetapir uptake, suggesting that both tracers may be promising tools to visualize cardiac amyloid involvement. Furthermore, these authors suggest that based on cardiac [^{18}F]-florbetapir retention index, ATTR patients could be distinguished from AL patients. A disadvantage of the use of these PET techniques is the need for dynamic imaging during 60 min after injection. Furthermore, quantification is a laborious process.

The case report describes the successful use of [^{11}C]-BF-227 in identifying cardiac amyloid deposits in a patient with ATTR amyloidosis and comparing the tracer uptake to a healthy control subject [24]. Finally, despite its value in localized extra-cardiac amyloidosis, [^{18}F]-FDG is of no value for cardiac involvement of systemic amyloidosis [25, 26].

Imaging cardiac sympathetic innervation

Myocardial adrenergic denervation, using [^{123}I]-MIBG, has been shown to be present in patients with amyloidosis [27–29]. In an indirect way, [^{123}I]-MIBG visualizes the effect of amyloid deposition in the myocardium. This technique might be able to detect early cardiac denervation before ongoing deposition of amyloid leads to actual heart failure.

Sympathetic nerve fibres interact with postsynaptic β -adrenergic receptors on the cell membrane of myocytes through norepinephrine. Norepinephrine is produced in the presynaptic nerve terminals and stored in presynaptic vesicles. After a stimulus, these vesicles release norepinephrine into the synaptic cleft and subsequently norepinephrine binds to the β -adrenergic receptors, resulting in cardiac stimulatory effects.

[^{123}I]-MIBG is the result of chemical modification of the false neurotransmitter analogue guanethidine and therefore an analogue of norepinephrine. The uptake of [^{123}I]-MIBG occurs similarly to the uptake of norepinephrine: predominantly by a specific uptake system (“uptake-1”) and to a much lesser extent by a non-specific uptake system (passive diffusion, “uptake-2”). Eventually, like norepinephrine, [^{123}I]-MIBG is stored in granules of presynaptic nerve terminals. In a normal situation, unlike norepinephrine, [^{123}I]-MIBG is not bound to receptors on the myocyte membrane and thus not catabolized by monoamine oxidase (MOA). Therefore, normally it is retained in these granules [30, 31].

At present, planar (anterior view, scanning time 3–5 min) images, preferable using a medium-energy collimator, are made 15 min as well as 3–5 h after administration of 111–300 (mean 185) MBq [^{123}I]-MIBG. The late planar images are often combined with SPECT images. A

semi-quantitative assessment of the heart-to-mediastinum ratio (HMR) is used to determine global uptake on the planar images. The wash-out rate between these images provides additional information and reflects the degree of sympathicotonia [32, 33]. Although normal values for HMR and wash-out rates seem to vary between age and image acquisition, HMR values <1.6 as well as wash-out rates >20 % indicate cardiac denervation [34].

The acquisition of SPECT has advantages for evaluating abnormalities in regional distribution in the myocardium [27–29, 35–37]. Usually, the reconstructed data are displayed in three planes (short axis, horizontal long axis and vertical long axis), which is similar to that used in myocardial perfusion SPECT.

Analogues to myocardial perfusion imaging, the use of polar maps can be used to calculate extent and severity scores for segmental defects. Comparing perfusion imaging to [¹²³I]-MIBG distribution provides extra information about the presence or absence of mismatch patterns. Myocardial ischaemia or infarction disrupts sympathetic transmission, which may lead to denervation of a region larger than affected by ischaemia only. Furthermore, sympathetic nervous tissue is more sensitive to ischaemia than cardiomyocytes. The presence of innervation/perfusion imaging mismatches correlates with electrophysiological abnormalities and increasing inducibility of potential lethal dysrhythmia [38, 39].

[¹²³I]-MIBG in cardiac amyloidosis

The use of [¹²³I]-MIBG is studied most intensively in patients with hereditary ATTR amyloidosis with polyneuropathy. The first reported cases showed no uptake in the heart on either early or late images, indicating severe impairment of cardiac sympathetic function [27, 35]. Subsequent larger studies of patients with biopsy-proven cardiac amyloidosis confirmed these findings. In some studies, these patients also underwent rest myocardial perfusion scintigraphy using Thallium-201. Patients with hereditary ATTR amyloidosis and polyneuropathy were found to have a high incidence of myocardial adrenergic denervation despite normal myocardial perfusion, LV function, and viability, which can be found early in cardiac amyloidosis in the absence of clinically apparent heart disease (Figs. 1, 2) [28, 29].

Furthermore, progression of sympathetic denervation seems to stop after liver transplantation, since the HMR before and after liver transplantation appeared to be not different [36]. In this same study, early re-innervation could not be measured within 2 years after liver transplantation. However, conduction disturbances, ventricular arrhythmias, and LV wall thickening were associated with low [¹²³I]-MIBG uptake and progressed after liver

transplantation. This may implicate progression of cardiac amyloid infiltration after liver transplantation [40].

Compared to other imaging modalities for cardiac involvement of amyloidosis, especially echocardiography, [¹²³I]-MIBG scintigraphy seems to be able to detect these signs in an earlier stage of the disease [7]. In this study, late HMR was significantly lower and wash-out rates were significantly higher in patients with echocardiographic signs of amyloidosis than in patients without these signs. Furthermore, in ATTR patients with polyneuropathy but without echocardiographic signs of amyloidosis, HMR was lower than in patients with other types of amyloidosis (AL and AA).

The most recent and largest study in ATTR patients showed that late HMR was an independent prognostic predictor of all-cause mortality [41]. The 5-year mortality rate in patients with low HMR was 42 %, compared to 7 % in patients with normal HMR. Eventually 53 of the 143 included patients underwent liver transplantation. Long-term mortality in this subgroup was reduced (total group: hazard ratio 0.32, $p = 0.012$), even in those patients with a high risk of unfavourable outcome based on low HMR. Therefore, [¹²³I]-MIBG scintigraphy can also be used as a prognostic tool in ATTR patients.

The use of [¹²³I]-MIBG in only patients with AL-type amyloidosis has hardly been studied. In fact only one major study has been performed in which the presence of impaired myocardial sympathetic innervation was related to clinical autonomic abnormalities and congestive heart failure in AL amyloidosis [37]. In this study, 25 patients with biopsy-proven cardiac manifestation of AL amyloidosis underwent autonomic function tests, echocardiography, heart rate variability analysis, and [¹²³I]-MIBG scanning. In patients with autonomic dysfunction, HMR and wash-out rates were significantly decreased compared to the patients without autonomic dysfunction. HMR was significantly decreased and wash-out rate increased in patients with heart failure compared to the patients without heart failure. Therefore, myocardial uptake and turnover of [¹²³I]-MIBG in patients with AL amyloidosis are heterogeneous and seem to depend on the presence of both congestive heart failure and cardiac autonomic dysfunction.

We are not aware of studies performed in which only patients with AA amyloidosis were scanned using [¹²³I]-MIBG for the detection of cardiac denervation.

Applications of nuclear imaging in the overall clinical spectrum of cardiac amyloidosis

From the above review, it is evident that the contribution of nuclear medicine imaging modalities, albeit consistent and

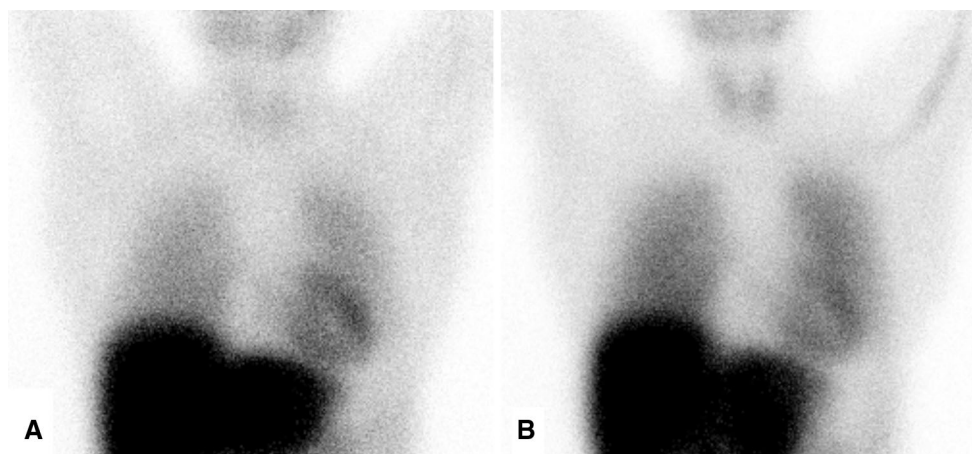


Fig. 1 Normal [^{123}I]-MIBG scintigraphy in a patient with AL amyloidosis: **a** early image acquired after 15 min after tracer administration, **b** late image acquired after 4 h post injection. Both

images show comparable tracer uptake. Early heart-to-mediastinum ratio (HMR) 1.8, late HMR 1.7, wash-out 7 %

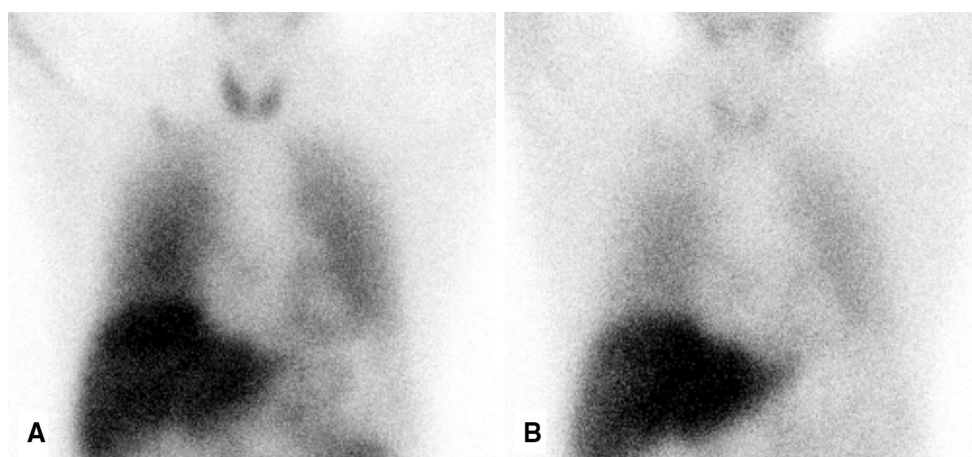


Fig. 2 Abnormal [^{123}I]-MIBG scintigraphy in a patient with ATTR amyloidosis. **a** Early image acquired after 15 min after tracer administration, **b** late image acquired after 4 h post injection.

a Shows normal tracer distribution, whereas **b** shows evident decrease in tracer accumulation. Early HMR 2.4, late HMR 1.8, wash-out 25 %

clinically relevant in general, varies considering the different radiopharmaceuticals and techniques, the different stages of the disease's history, and the heterogeneous clinical needs of the physician treating the patient with definite or suspected cardiac amyloidosis. Table 1 summarizes this variable diagnostic and prognostic contribution.

Patients with cardiac amyloidosis usually present with clinical signs and symptoms of right-sided heart failure, with progressive dyspnoea as the most common complaint [42]. The diagnosis is based on histological proof from endomyocardial biopsy, especially when amyloidosis is limited to the heart. But this gold standard is limited to centres with cardiopathology facilities, is an invasive procedure, and harbours a non-negligible risk of perforation and bleeding, and typing of amyloid is fraught with errors.

Identification of the aetiology has important consequences for the management of cardiac amyloidosis. To date, the gold standard for characterization of the underlying subtype, especially the differentiation between ATTR and AL, is laser microdissection and analytical power of tandem mass spectrometry-based proteomic analysis (LMD-MS) [43]. This differentiation is important, since in case of incorrect diagnosis of AL-type amyloidosis, chemotherapy may be given in error. Nuclear medicine modalities have the potential to visualize functional consequences of cardiac amyloid infiltration, are able to discriminate between AL- and ATTR-type amyloidosis with high diagnostic accuracy, and may also be able to monitor response to treatment (Table 1). Furthermore, results of these scans can have prognostic implications of the progression of heart failure.

Table 1 Overview of the most frequently used tracers for imaging cardiac amyloidosis and their clinical aims

Clinical aim	Diphosphonates		PET tracers		¹²³ I-MIBG
	(^{99m} Tc-DPD/MDP/HDP)	^{99m} Tc-pyrophosphate	¹⁸ F-florbetapir	¹¹ C-PiB	
Physiological mechanism	Amyloid deposits in the heart	Amyloid deposits in the heart	β-amyloid deposits	β-amyloid deposits	Cardiac sympathetic innervation
Soft tissue infiltration	+	?	+	+	–
Myocardial infiltration	+++	++	++ (?)	++ (?)	–
Early myocardial involvement	+++	?	?	?	+
ATTR versus AL	+++	++	++ (?)	–	–
Cardiac sympathetic denervation	–	–	–	–	++
Quantification of amyloidotic burden	++	+ (?)	?	?	–
Response to therapy	+ (?)	?	?	?	?
Prognostic stratification	++	?	?	?	+

Legend: ? unknown, or not enough evidence; – not applicable; + moderately applicable; ++ good applicable; +++ very good applicable

Functional consequences of amyloid infiltration can be divided in vascular problems, systolic and diastolic dysfunction, and conduction and rhythm disorders. Amyloidotic infiltration in the coronary arteries is a known complication of systemic amyloidosis [44]. Consequences of this vascular infiltration are not fully elucidated. Patients can present with atypical chest discomfort; however, this was previously considered to be related to heart failure instead of myocardial ischaemia [42, 44]. Conventional myocardial perfusion scintigraphy can be negative in patients with cardiac amyloidosis. However, a myocardial perfusion—sympathetic mismatch pattern (normal perfusion with a defect on [¹²³I]-MIBG scintigraphy)—may indicate microvascular dysfunction as a result of coronary amyloid deposits. The presence of microvascular dysfunction in patients with cardiac amyloidosis was recently further established [45]. Twenty-one patients with cardiac amyloidosis but without epicardial coronary artery disease, and ten disease-control patients underwent myocardial perfusion PET. The amyloidosis patients showed lower myocardial blood flow and lower flow reserve, which could be explanations for symptoms of chest pain.

Diastolic dysfunction is the most important functional consequence, since it is the hallmark of restrictive cardiomyopathy. Echocardiography is the modality of choice to assess transmitral inflow. Radionuclide ventriculography, or multiple gated acquisition (MUGA), also has the potential to quantify for example time-to-peak filling and peak filling rate [46]. However, this requires a special acquisition and an experienced reader for interpretation. For determining systolic function, MUGA can still be

considered the gold standard. Echocardiography and MRI generally show similar results.

Syncope can be considered as a clinical presentation of different types of conduction problems and arrhythmia. First, it may be a consequence of bradycardia due to amyloid infiltration in the conduction system. Secondly, syncope can be a result of sustained ventricular tachycardia. Third, it may be caused by hypotension due to autonomic neuropathy or forward failure, sometimes aggravated by overuse of diuretic drugs. Finally, it may be the onset of sudden cardiac death due to electromechanical dissociation rather than ventricular arrhythmia [47]. Nuclear medicine modalities are not able to visualize the actual amyloid deposits in the conduction system. However, sympathetic innervation abnormalities assessed by [¹²³I]-MIBG scintigraphy can be considered as a consequence of amyloid infiltration in the sympathetic nerve system [27]. Furthermore, the aforementioned perfusion–innervation mismatch can be considered as a risk factor for developing ventricular arrhythmia.

Quantification of amyloidotic burden is an interesting development in nuclear medicine. Up to recently, only semi-quantitative assessment was possible for bone scintigraphy and [¹²³I]-MIBG scintigraphy. In bone scintigraphy, heart-to-whole body ratios can be determined using the total image counts corrected for kidney and bladder uptake and residual activity at the injection site considering as the whole-body uptake [8, 9, 16, 48]. Heart-to-skull ratio was also proposed, with potential advantages over heart-to-whole body ratios in those patients with other active osteoblastic diseases (Fig. 3) [16]. Both semi-quantitative

methods correlate with echocardiographic parameters for cardiac amyloidosis, and may even detect cardiac involvement before echocardiography does [16]. These semi-quantitative measurements may also be used to compare the uptake in the heart in time. As a consequence, it might be possible to monitor the results of therapy or give an indication when to start therapy as the uptake is increasing in time.

As stated before, HMR assessed by [^{123}I]-MIBG scintigraphy may also show cardiac involvement before echocardiographic parameters are positive [7]. Furthermore, low HMR has shown to have prognostic consequences in terms of 5-year survival [41]. Absolute quantification of cardiac amyloidotic burden is now possible with the first

application of PET tracers [6, 23]. However, the prognostic value of retention indices has to be determined in larger clinical trials.

Future developments

There is an increasing need for (consensus-based) guidelines for image acquisition and image-based clinical decision making in patients with cardiac amyloidosis, especially in those patients with negative results on echocardiography. Furthermore, it is important to further explore the diagnostic value of serial bone scintigraphy in quantification, and to determine its role in disease progression and response to treatment in ATTR patients.

The introduction of hybrid camera systems makes superposition of physiological and anatomical information possible. The simultaneous acquisition of PET and MRI is the most recent development in medical imaging. Evaluation of cardiac amyloidosis has the potential to become a unique application for PET/MRI, in which either modality provides complementary information, especially since the introduction of novel MRI sequences as non-contrast T1 mapping [49]. PET tracer retention at the location of sub-endocardial delayed gadolinium enhancement or non-contrast T1 mapping may increase the positive predictive value of the presence of cardiac amyloidosis on either PET or MRI.

Finally, the combination of nuclear medicine modalities with proteomics may be a field worthwhile for exploration. In the subtypes of amyloidosis, different proteins are both upregulated and downregulated. The background of this alteration is yet not entirely clear and could either be reactive due to the disease or related to amyloid deposits in the microenvironment of the extracellular space. Proteomics may teach us about the specific composition of amyloid and surrounding tissue in order to develop new tracers that specifically target cardiac amyloid [50, 51]. Realizing unambiguous imaging of cardiac amyloid may fill two great clinical needs: early disease detection and reliable monitoring of a treatment effect. Targeting these proteins and visualizing their distribution in the body may lead to new insights within amyloidosis in general.

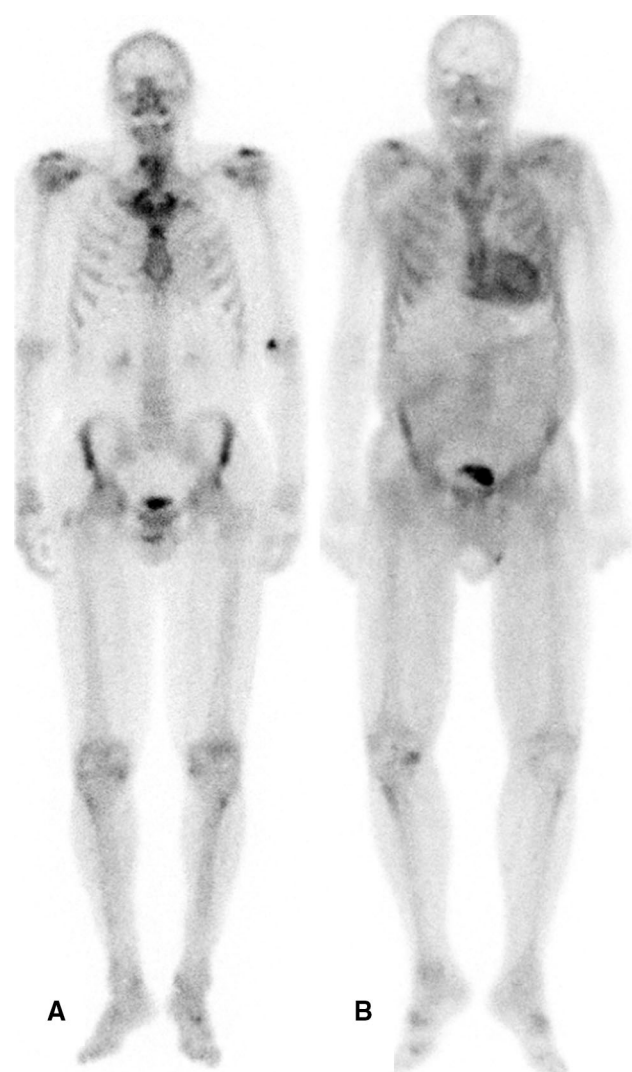


Fig. 3 Comparison of [$^{99\text{m}}\text{Tc}$]-hydroxy-methylene diphosphonate distribution in elderly patients with AL (**a**, no cardiac uptake) and ATTR amyloidosis (**b**, intense cardiac accumulation). Both images furthermore show uptake in degenerative changes and physiological excretion through the urinary tract

Conclusion

Nuclear medicine modalities are well established in the work-up of patients with cardiac amyloidosis and are of value in the non-invasive assessment of early diagnosis, underlying subtype, prognostic consequences and—in the future—probably also for therapy evaluation.

Conflict of interest Dr. Noordzij, Dr. Glaudemans, Dr. Longhi, Dr. Slart, Dr. Lorenzini, Dr. Hazenberg and Dr. Rapezzi have no conflict of interest or financial ties to disclose.

Ethics standard This manuscript does not contain unpublished clinical studies or new patient data.

References

- Hamer JP, Janssen S, van Rijswijk MH, Lie KI (1992) Amyloid cardiomyopathy in systemic non-hereditary amyloidosis. Clinical, echocardiographic and electrocardiographic findings in 30 patients with AA and 24 patients with AL amyloidosis. *Eur Heart J* 13:623–627
- Hazenberg BP, van Rijswijk MH, Piers DA, Lub-de Hooge MN, Vellenga E, Haagsma EB, Hawkins PN, Jager PL (2006) Diagnostic performance of 123I-labeled serum amyloid P component scintigraphy in patients with amyloidosis. *Am J Med* 119:355.e15–355.e24
- Aprile C, Marinone G, Saponaro R, Bonino C, Merlini G (1995) Cardiac and pleuropulmonary AL amyloid imaging with technetium-99m labelled aprotinin. *Eur J Nucl Med* 22:1393–1401
- Wall JS, Kennel SJ, Stuckey AC, Long MJ, Townsend DW, Smith GT, Wells KJ, Fu Y, Stabin MG, Weiss DT, Solomon A (2010) Radioimmunodetection of amyloid deposits in patients with AL amyloidosis. *Blood* 116:2241–2244
- Rapezzi C, Quarta CC, Guidalotti PL, Longhi S, Pettinato C, Leone O, Ferlini A, Salvi F, Gallo P, Gagliardi C, Branzi A (2011) Usefulness and limitations of 99mTc-3,3-diphosphono-1,2-propanodicarboxylic acid scintigraphy in the aetiological diagnosis of amyloidotic cardiomyopathy. *Eur J Nucl Med Mol Imaging* 38:470–478
- Antoni G, Lubberink M, Estrada S, Axelsson J, Carlson K, Lindsjö L, Kero T, Långström B, Granstam SO, Rosengren S, Vedin O, Wassberg C, Wikström G, Westermark P, Sörensen J (2013) In vivo visualization of amyloid deposits in the heart with 11C-PIB and PET. *J Nucl Med* 54:213–220
- Noordzij W, Glaudemans AW, van Rheenen RW, Hazenberg BP, Tio RA, Dierckx RA, Slart RH (2012) (123I)-Labelled metaiodobenzylguanidine for the evaluation of cardiac sympathetic denervation in early stage amyloidosis. *Eur J Nucl Med Mol Imaging* 39:1609–1617
- Kula RW, Engel WK, Line BR (1977) Scanning for soft-tissue amyloid. *Lancet* 1:92–93
- Puille M, Altland K, Linke RP, Steen-Müller MK, Kiett R, Steiner D, Bauer R (2002) 99mTc-DPD scintigraphy in transthyretin-related familial amyloidotic polyneuropathy. *Eur J Nucl Med Mol Imaging* 29:376–379
- Perugini E, Guidalotti PL, Salvi F, Cooke RM, Pettinato C, Riva L, Leone O, Farsad M, Ciliberti P, Bacchi-Reggiani L, Fallani F, Branzi A, Rapezzi C (2005) Noninvasive etiologic diagnosis of cardiac amyloidosis using 99mTc-3,3-diphosphono-1,2-propanodicarboxylic acid scintigraphy. *J Am Coll Cardiol* 46:1076–1084
- Rapezzi C, Quarta CC, Guidalotti PL, Pettinato C, Fanti S, Leone O, Ferlini A, Longhi S, Lorenzini M, Reggiani LB, Gagliardi C, Gallo P, Villani C, Salvi F (2011) Role of (99m)Tc-DPD scintigraphy in diagnosis and prognosis of hereditary transthyretin-related cardiac amyloidosis. *JACC Cardiovasc Imaging* 4:659–670
- Longhi S, Guidalotti PL, Quarta CC, Gagliardi C, Milandri A, Lorenzini M, Potena L, Leone O, Bartolomei I, Pastorelli F, Salvi F, Rapezzi C (2014) Identification of TTR-related subclinical amyloidosis with 99mTc-DPD scintigraphy. *JACC Cardiovasc Imaging* 7:531–532
- Hutt DF, Quigley AM, Page J, Hall ML, Burniston M, Gopaul D, Lane T, Whelan CJ, Lachmann HJ, Gillmore JD, Hawkins PN, Wechalekar AD (2014) Utility and limitations of 3,3-diphosphono-1,2-propanodicarboxylic acid scintigraphy in systemic amyloidosis. *Eur Heart J Cardiovasc Imaging* 15:1289–1298
- Frühling J, Verbist A, Balikdjian D (1986) Which diphosphonate for routine bone scintigraphy (MDP, HDP or DPD)? *Nucl Med Commun* 7:415–425
- Pauwels EK, Blom J, Camps JA, Hermans J, Rijke AM (1983) A comparison between the diagnostic efficacy of 99mTc-MDP, 99mTc-DPD and 99mTc-HDP for the detection of bone metastases. *Eur J Nucl Med* 8:118–122
- Glaudemans AW, van Rheenen RW, van den Berg MP, Noordzij W, Koole M, Blokzijl H, Dierckx RA, Slart RH, Hazenberg BP (2014) Bone scintigraphy with (99m)technetium-hydroxymethylene diphosphonate allows early diagnosis of cardiac involvement in patients with transthyretin-derived systemic amyloidosis. *Amyloid* 21:35–44
- Falk RH, Lee VW, Rubinow A, Hood WB Jr, Cohen AS (1983) Sensitivity of technetium-99m-pyrophosphate scintigraphy in diagnosing cardiac amyloidosis. *Am J Cardiol* 51:826–830
- Lee VW, Caldarone AG, Falk RH, Rubinow A, Cohen AS (1983) Amyloidosis of heart and liver: comparison of Tc-99m pyrophosphate and Tc-99m methylene diphosphonate for detection. *Radiology* 148:239–242
- Eriksson P, Backman C, Bjerle P, Eriksson A, Holm S, Olofsson BO (1984) Non-invasive assessment of the presence and severity of cardiac amyloidosis. A study in familial amyloidosis with polyneuropathy by cross sectional echocardiography and technetium-99m pyrophosphate scintigraphy. *Br Heart J* 52:321–326
- Janssen S, Piers DA, van Rijswijk MH, Meijer S, Mandema E (1990) Soft-tissue uptake of 99mTc-diphosphonate and 99mTc-pyrophosphate in amyloidosis. *Eur J Nucl Med* 16:663–670
- Yamamoto Y, Onoguchi M, Haramoto M, Kodani N, Komatsu A, Kitagaki H, Tanabe K (2012) Novel method for quantitative evaluation of cardiac amyloidosis using (201)TlCl and (99m)Tc-PYP SPECT. *Ann Nucl Med* 26:634–643
- Bokhari S, Castaño A, Pozniakoff T, Deslisle S, Latif F, Maurer MS (2013) (99m)Tc-pyrophosphate scintigraphy for differentiating light-chain cardiac amyloidosis from the transthyretin-related familial and senile cardiac amyloidoses. *Circ Cardiovasc Imaging* 6:195–201
- Dorbala S, Vangala D, Semer J, Strader C, Bruyere JR Jr, Di Carli MF, Moore SC, Falk RH (2014) Imaging cardiac amyloidosis: a pilot study using 18F-florbetapir positron emission tomography. *Eur J Nucl Med Mol Imaging* 41:1652–1662
- Furukawa K, Ikeda S, Okamura N, Tashiro M, Tomita N, Furumoto S, Iwata R, Yanai K, Kudo Y, Arai H (2012) Cardiac positron-emission tomography images with an amyloid-specific tracer in familial transthyretin-related systemic amyloidosis. *Circulation* 125:556–557
- Glaudemans AW, Slart RH, Noordzij W, Dierckx RA, Hazenberg BP (2013) Utility of 18F-FDG PET/CT in patients with systemic and localized amyloidosis. *Eur J Nucl Med Mol Imaging* 40:1095–1101
- Mekinian A, Jaccard A, Soussan M, Launay D, Berthier S, Federici L, Lefèvre G, Valeyre D, Dhote R, Fain O (2012) 18F-FDG PET/CT in patients with amyloid light-chain amyloidosis: case-series and literature review. *Amyloid* 19:94–98
- Nakata T, Shimamoto K, Yonekura S, Sugiyama T, Imai K, Imura O (1995) Cardiac sympathetic denervation in transthyretin-related familial amyloidotic polyneuropathy: detection with iodine-123-MIBG. *J Nucl Med* 36:1040–1042

28. Tanaka M, Hongo M, Kinoshita O, Takabayashi Y, Fujii T, Yazaki Y, Isobe M, Sekiguchi M (1997) Iodine-123 metaiodobenzylguanidine scintigraphic assessment of myocardial sympathetic innervation in patients with familial amyloid polyneuropathy. *J Am Coll Cardiol* 29:168–174
29. Delahaye N, Dinanian S, Slama MS, Mzabi H, Samuel D, Adams D, Merlet P, Le Guludec D (1999) Cardiac sympathetic denervation in familial amyloid polyneuropathy assessed by iodine-123 metaiodobenzylguanidine scintigraphy and heart rate variability. *Eur J Nucl Med* 26:416–424
30. Kline RC, Swanson DP, Wieland DM, Thrall JH, Gross MD, Pitt B, Beierwaltes WH (1981) Myocardial imaging in man with I-123 metaiodobenzylguanidine. *J Nucl Med* 22:129–132
31. Wieland DM, Brown LE, Rogers WL, Worthington KC, Wu JL, Clinthorne NH, Otto CA, Swanson DP, Beierwaltes WH (1981) Myocardial imaging with a radioiodinated norepinephrine storage analog. *J Nucl Med* 22:22–31
32. Somsen GA, Verberne HJ, Fleury E, Righetti A (2004) Normal values and within-subject variability of cardiac I-123 MIBG scintigraphy in healthy individuals: implications for clinical studies. *J Nucl Cardiol* 11:126–133
33. Ogita H, Shimonagata T, Fukunami M, Kumagai K, Yamada T, Asano Y, Hirata A, Asai M, Kusuoka H, Hori M, Hoki N (2001) Prognostic significance of cardiac 123I metaiodobenzylguanidine imaging for mortality and morbidity in patients with chronic heart failure: a prospective study. *Heart* 86:656–660
34. Jacobson AF, Lombard J, Banerjee G, Camici PG (2009) 123I-MIBG scintigraphy to predict risk for adverse cardiac outcomes in heart failure patients: design of two prospective multicenter international trials ADMIRE-HF study. *J Nucl Cardiol* 16:113–121
35. Arbab AS, Koizumi K, Toyama K, Arai T, Yoshitomi T, Araki T (1997) Scan findings of various myocardial SPECT agents in a case of amyloid polyneuropathy with suspected myocardial involvement. *Ann Nucl Med* 11:139–141
36. Delahaye N, Rouzet F, Sarda L, Tamas C, Dinanian S, Plante-Bordeneuve V, Adams D, Samuel D, Merlet P, Syrota A, Slama MS, Le Guludec D (2006) Impact of liver transplantation on cardiac autonomic denervation in familial amyloid polyneuropathy. *Medicine* 85:229–238
37. Hongo M, Urushibata K, Kai R, Takahashi W, Koizumi T, Uchikawa S, Imamura H, Kinoshita O, Owa M, Fujii T (2002) Iodine-123 metaiodobenzylguanidine scintigraphic analysis of myocardial sympathetic innervation in patients with AL (primary) amyloidosis. *Am Heart J* 144:122–129
38. Simões MV, Barthel P, Matsunari I, Nekolla SG, Schömig A, Schwaiger M, Schmidt G, Bengel FM (2004) Presence of sympathetically denervated but viable myocardium and its electrophysiologic correlates after early revascularised, acute myocardial infarction. *Eur Heart J* 25:551–557
39. Sasano T, Abraham R, Chang KC, Ashikaga H, Mills KJ, Holt DP, Hilton J, Nekolla SG, Dong J, Lardo AC, Halperin H, Dannals RF, Marbán E, Bengel FM (2008) Abnormal sympathetic innervation of viable myocardium and the substrate of ventricular tachycardia after myocardial infarction. *J Am Coll Cardiol* 51:2266–2275
40. Haagsma EB, van Gameren II, Bijzet J, Posthumus MD, Hazenberg BP (2007) Familial amyloidotic polyneuropathy: long-term follow-up of abdominal fat tissue aspirate in patients with and without liver transplantation. *Amyloid* 14:221–226
41. Coutinho MC, Cortez-Dias N, Cantinho G, Conceição I, Oliveira A, Bordalo e Sá A, Gonçalves S, Almeida AG, de Carvalho M, Diogo AN (2013) Reduced myocardial 123-Iodine metaiodobenzylguanidine uptake: a prognostic marker in familial amyloid polyneuropathy. *Circ Cardiovasc Imaging* 6:627–636
42. Dubrey SW, Cha K, Anderson J, Chamathi B, Reisinger J, Skinner M, Falk RH (1998) The clinical features of immunoglobulin light-chain (AL) amyloidosis with heart involvement. *QJM* 91:141–157
43. Vrana JA, Gamez JD, Madden BJ, Theis JD, Bergen HR 3rd, Dogan A (2009) Classification of amyloidosis by laser microdissection and mass spectrometry-based proteomic analysis in clinical biopsy specimens. *Blood* 114:4957–4959
44. Mueller PS, Edwards WD, Gertz MA (2000) Symptomatic ischemic heart disease resulting from obstructive intramural coronary amyloidosis. *Am J Med* 109:181–188
45. Dorbala S, Vangala D, Bruyere J Jr, Quarta C, Kruger J, Padera R, Foster C, Hanley M, Di Carli MF, Falk R (2014) Coronary microvascular dysfunction is related to abnormalities in myocardial structure and function in cardiac amyloidosis. *JACC Heart Fail* 2:358–367
46. Mitra D, Basu S (2012) Equilibrium radionuclide angiocardiology: its usefulness in current practice and potential future applications. *World J Radiol* 4:421–430
47. Falk RH, Rubinow A, Cohen AS (1984) Cardiac arrhythmias in systemic amyloidosis: correlation with echocardiographic abnormalities. *J Am Coll Cardiol* 3:107–113
48. Rapezzi C, Guidalotti P, Salvi F, Riva L, Perugini E (2008) Usefulness of 99mTc-DPD scintigraphy in cardiac amyloidosis. *J Am Coll Cardiol* 51:1509–1510
49. Karamitsos TD, Piechnik SK, Banyersad SM, Fontana M, Ntusi NB, Ferreira VM, Whelan CJ, Myerson SG, Robson MD, Hawkins PN, Neubauer S, Moon JC (2014) Noncontrast T1 mapping for the diagnosis of cardiac amyloidosis. *JACC Cardiovasc Imaging* 6:488–497
50. Brambilla F, Lavatelli F, Di Silvestre D, Valentini V, Palladini G, Merlini G, Mauri P (2013) Shotgun protein profile of human adipose tissue and its changes in relation to systemic amyloidosis. *J Proteome Res* 12:5642–5655
51. Di Silvestre D, Brambilla F, Mauri PL (2013) Multidimensional protein identification technology for direct-tissue proteomics of heart. *Method Mol Biol* 1005:25–38